

Micron- and submicron-sized surface patterning of silica glass by LIBWE method

Ximing Ding, Yoshizo Kawaguchi, Tadatake Sato,
Aiko Narazaki, Ryozo Kurosaki, Hiroyuki Niino*

*Phonics Research Institute, National Institute of Advanced Industrial Science and Technology (AIST),
Tsukuba Central 5, 1-1-1 Higashi, Tsukuba, Ibaraki 305-8565, Japan*

Received 8 December 2003; received in revised form 22 January 2004; accepted 5 April 2004

Abstract

Microstructures with well-defined 1 μm -scale grating and grid patterns were fabricated on the surfaces of silica glass using a laser-induced backside wet etching (LIBWE) method by nanosecond-pulsed KrF excimer laser irradiation through a mask projection system. In the former case, gratings as narrow as 0.75 μm -sized were successfully etched on the glass surface via fine adjustments to the projection system. To investigate the etching mechanisms, formation and propagation of the shockwave and micro-bubbles after laser irradiation, at the interface of the silica glass and the toluene solution, were monitored using time-resolved shadowgraph microscopy, from the front- and side-view directions.

© 2004 Elsevier B.V. All rights reserved.

Keywords: Silica glass; Surface micro-structuring; Ablation; Nanosecond-pulsed UV laser; Shockwave; Micro-bubble; Time-resolved shadowgraph microscopy

1. Introduction

Laser-induced micro-fabrication of various materials has served as an important technique in surface structuring for optics and optoelectronic devices [1]. In particular, significant attention has been given towards the micro-fabrication of silica glass, since, in spite of the difficulty involved, silica is a commonly used material. The use of pulsed lasers can involve several approaches, such as conventional UV laser ablation [2], vacuum UV laser processing [3,4], plasma-assisted UV ablation [5,6], and femtosecond laser micromachining [2,7].

Recently, we have demonstrated a novel one-step method, laser-induced backside wet etching (LIBWE), for micro-fabrication on a silica glass plate, involving irradiation with a nanosecond-pulsed UV excimer laser [8–24]. The LIBWE method is based on the deposition of laser energy onto a thin layer at the glass-liquid interface during the ablation of a liquid substance. The experimental setup for the LIBWE method is shown in Fig. 1. Assuming negligible UV absorption by the silica glass, the incident laser beam passes through the glass plate resulting in the excitation of

the dye solution. If the dye solution becomes ablated using laser irradiation with sufficient fluence, etching on a surface layer of the silica glass is achieved. The depth of the etch increases linearly with the number of laser shots. Typical etch rates of the material were 0.1–25 nm per pulse, depending on various irradiation conditions such as laser wavelength, laser fluence, and dye concentrations. Micro-fabrications of various transparent materials, such as silica glass [8,11–13,17–21], quartz [9,19,22–24], glasses (Pyrex, etc.) [20], calcium fluoride [11,19,24], magnesium fluoride [19], barium fluoride [24], fluorocarbon resin [10], and sapphire [16,19,24], have been reported. Furthermore, various dye solutions, such as pyrene/acetone [8,9,11,12,16,17,19–23], pyrene/tetrahydrofuran (THF) [10], pyrene/tetrachloroethylene [19,20,22], pyrene/cyclohexane [19], pyrene/toluene [20–22], pyranine/water [13], naphthalenesulfonic acid/water [14], and pure toluene [15,18], have been used in conjunction with irradiation with KrF, XeCl, and XeF excimer lasers.

In this paper, we report on the fabrication of various micro-patterns on silica glass using the LIBWE method with a mask projection system. Additionally, to observe dynamics in liquid ablation, time-resolved optical shadowgraph measurements were carried out from the front and side directions. Transient shockwave and vapor micro-bubbles were

* Corresponding author. Tel.: +81 29 861 4562; fax: +81 29 861 4560.
E-mail address: niino.hiro@aist.go.jp (H. Niino).

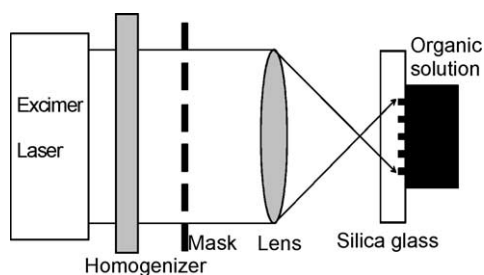


Fig. 1. Schematic diagram of the experimental setup for the LIBWE method.

observed following laser irradiation, suggesting that high pressure and temperature are induced on the surface of the glass materials by laser irradiation.

2. Experimental

A transparent synthetic silica glass plate (Tosoh SGM Co., ES grade) with a thickness of about 2 mm and a diameter of 20 mm was used as a sample. Naphthalene-1,3,6-trisulfonic acid trisodium salt was purchased from Tokyo Kasei. On

the basis of single photon absorption, the molar absorption coefficient (ϵ) of aqueous solution of naphthalene at a wavelength of 248 nm was $\epsilon = 3.15 \times 10^3 \text{ mol}^{-1} \text{ dm}^3 \text{ cm}^{-1}$. At 248 nm, the penetration depth of the solution at a concentration of 1.0 M was estimated as 3.2 μm .

A KrF laser (Lambda Physik, EMG201MSC, $\lambda = 248 \text{ nm}$, FWHM 30 ns) was used as the light source. The repetition rate of the laser irradiations was set at 5 Hz. As shown in Fig. 1, the aqueous solutions were in contact with one side of the plate, whereas the laser beam was introduced, at ambient temperatures, from the opposite side. Chromium-on-quartz-masks having grating and grid patterns were used to etch line-and-space and grid patterns, respectively. Grating and grid micro-patterns were projected onto the surface of silica glass plates using a demagnification ($8\times$) objective lens and homogenizer (Microlas Laser System). The morphology of etched patterns was analyzed using a confocal scanning laser microscope (Keyence, VK-8500).

The transient optical images of toluene ablation were monitored using time-resolved shadowgraph technique [14,15,25]. The solution in a quartz cubic cell was irradiated with a KrF laser through a single pinhole. For the side-view observation, the irradiated area was a circle with a diameter of 170 μm ; for the front-view, the area was a 250 $\mu\text{m} \times 250 \mu\text{m}$. The back illumination was provided by a dye solution (Rhodamine B in ethanol) excited with a XeCl laser providing a peak emission at 560 nm with a duration of 25 ns. Delay times between the KrF and XeCl lasers were regulated using a digital delay and pulse generator (Stanford Research Systems, DG535). By changing the delay times, time-resolved images of the ablation process were obtained using a conventional CCD-camera (Nikon, Coolpix 990) through an optical microscope (Mitsutoyo, M Plan Apo). Moreover, time-integrated UV–vis

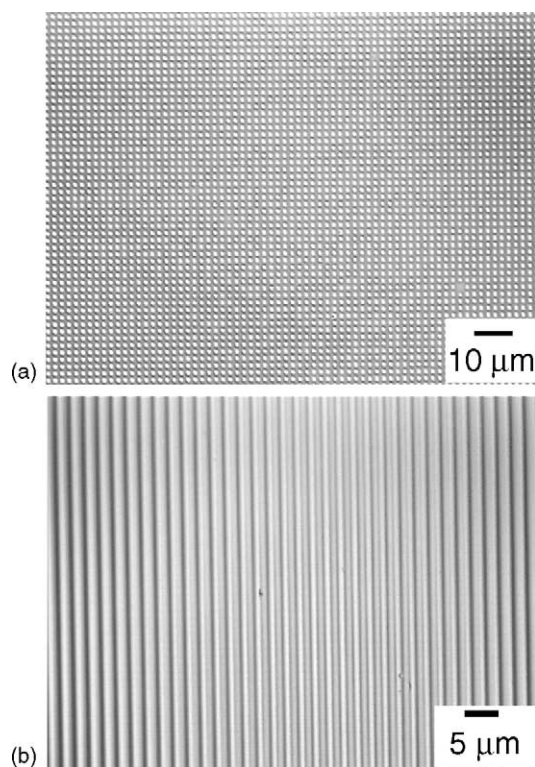


Fig. 2. Confocal scanning laser microscopic images of the etched patterns on the surface of a silica glass plate fabricated using an aqueous solution of a naphthalene derivative: (a) a $1 \mu\text{m} \times 1 \mu\text{m}$ grid pattern with an array of holes, fabricated by 1000 pulses of KrF irradiation at 1.6 J cm^{-2} using a 1.0 M aqueous dye solution, (b) $1 \mu\text{m}$ line-and-space patterns, fabricated by 6000 pulses of KrF irradiation at 1.6 J cm^{-2} using a 0.4 M aqueous dye solution.

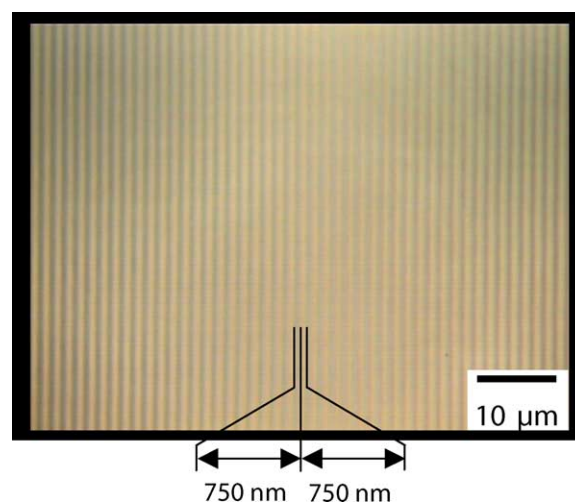


Fig. 3. Confocal scanning laser microscopic image of the etched grating pattern on the surface of a fused silica plate fabricated by 400 pulses of KrF irradiation at 1.0 J cm^{-2} and 4 Hz using a solution of pyrene in acetone with a concentration of 0.5 mol dm^{-3} .

emission spectrum of toluene, excited by KrF excimer laser irradiation, was recorded using a spectrophotometer (Hamamatsu, PMA-11) equipped with a UV cut-off filter.

3. Results and discussion

3.1. Submicron fabrication of silica glass

A $1\text{ }\mu\text{m} \times 1\text{ }\mu\text{m}$ grid pattern with an array of holes on the surface of a silica glass plate is shown in Fig. 2(a). The etched micro-pattern was fabricated using 1000 pulses of KrF irradiation at 1.6 J cm^{-2} and an aqueous 1.0 M solution of a naphthalene derivative (as the dye solution). The resulting micro-pattern was analyzed using a confocal scanning laser microscope. Although the etched holes were not perfectly square, which may simply be due to the resolution of the optical setup, the successful fabrication of such small holes on fused silica plates is a major breakthrough within laser micro-processing techniques. A fine line-and-space micro-pattern, on a $1\text{ }\mu\text{m}$ scale, was fabricated using 6000 pulses of KrF irradiation at 1.6 J cm^{-2} and an aqueous 0.4 M solution of the dye; its surface morphology is displayed in Fig. 2(b).

Moreover, the micro-fabrication of a $0.75\text{ }\mu\text{m} + 0.75\text{ }\mu\text{m}$ line-and-space grating micro-pattern was carried out via fine adjustments of the focal point of the projection system, as shown in Fig. 3. The depth of the wavy structure in the grating was estimated as 100 nm. In addition, both the top and bottom of the newly fabricated grating areas were etched during the LIBWE process because the resolving power of our projection system was not sufficient for the formation of the pattern at $0.75\text{ }\mu\text{m}$ resolution. The depth of the etched levels was approximately $2.4\text{ }\mu\text{m}$.

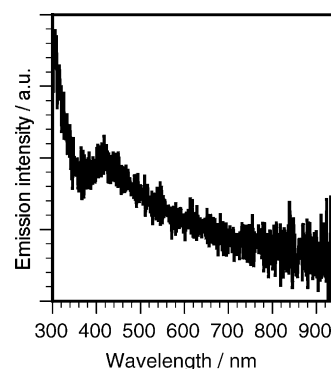


Fig. 5. Emission spectrum of pure toluene excited by KrF excimer laser irradiation at 1.6 J cm^{-2} .

Using a phase grating projection system equipped with a Schwarzschild objective, surface relief grating at sub-micron levels with a 787 nm grating period was successfully fabricated on fused silica [20]. An important advantage of our mask projection method is its ability to process relatively large areas (as large as $1\text{ mm} \times 1\text{ mm}$ or $2\text{ mm} \times 2\text{ mm}$).

3.2. In-situ observations of liquid ablation

In a previous paper [15], shockwave propagation and vapor expansion, which were induced by the explosive vaporization of the liquid ablation, were monitored from lateral directions of the incident laser beam using the shadowgraph technique for flash illumination. In our studies, observations were carried out from a different angle, after the laser irradiation of a $250\text{ }\mu\text{m} \times 250\text{ }\mu\text{m}$ square area.

The front-view images of toluene ablation, at delay times between 100 ns and $50\text{ }\mu\text{s}$ following KrF laser irradiation with a fluence of 1.6 J cm^{-2} are shown in Fig. 4. The formation of shockwave and vapor micro-bubble was observed

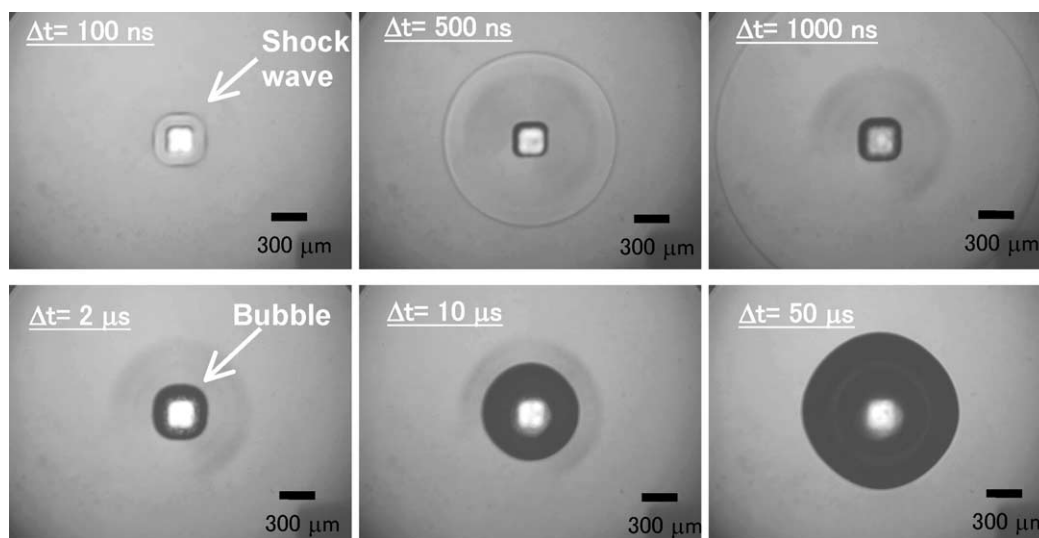


Fig. 4. Front-view images of toluene ablation obtained using time-resolved shadowgraph technique at a delay time (Δt) between 100 ns and $50\text{ }\mu\text{s}$ following irradiation using KrF excimer laser at 1.6 J cm^{-2} (laser beam size: $250\text{ }\mu\text{m} \times 250\text{ }\mu\text{m}$ square).

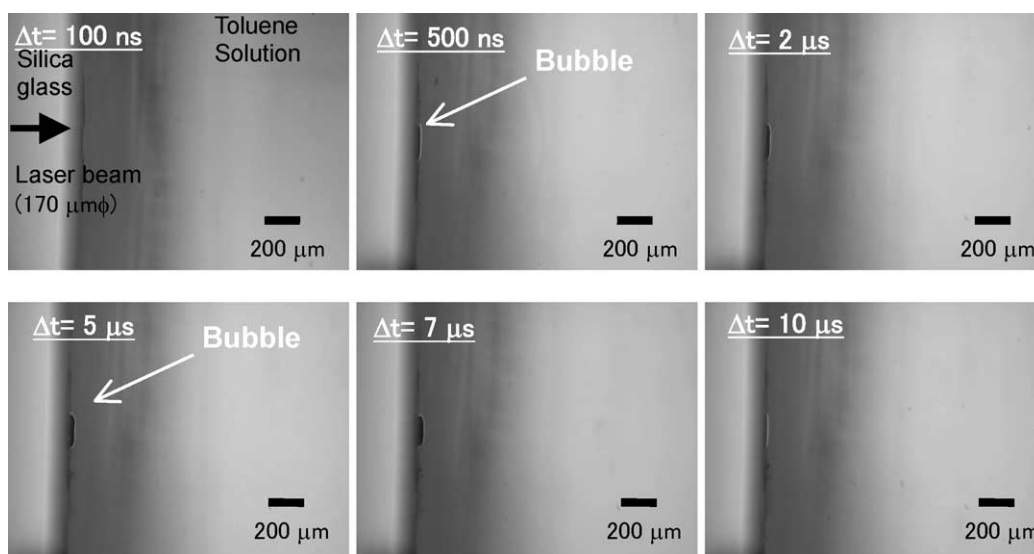


Fig. 6. Side-view images of toluene ablation obtained using time-resolved optical micrographic technique at a delay time (Δt) between 100 ns and 10 μ s following irradiation using KrF excimer laser at 100 mJ cm^{-2} (laser beam size: $170 \mu\text{m}$ diameter circle).

in the vicinity of the silica glass and toluene interface. Initial velocities of the expansion of the shockwaves and vapor micro-bubble were roughly 1.4 km s^{-1} and 200 m s^{-1} , respectively. After a delay time of $50 \mu\text{s}$, vapor expansion on the glass reached a maximum size of approximately $1300 \mu\text{m}$; the vapor dome shrunk gradually until $150 \mu\text{s}$. In the case of the $170 \mu\text{m}$ diameter irradiation at 1.6 J cm^{-2} [15], however, the maximum size of the micro-bubble was $600 \mu\text{m}$, and therefore, the maximum bubble size was dependent on the size of the laser irradiation. Since slower rates of thermal dissipation from the vapor micro-bubble during the expansion are expected for larger laser irradiation sizes, the maximum size of a $250 \mu\text{m} \times 250 \mu\text{m}$ square irradiation was significantly larger than that of a $170 \mu\text{m}$ diameter circle irradiation. This size-dependency in thermal dissipation is attributable to the ratio between the surface area and the volume during the expansion of the micro-bubble.

Both the front- and side-view observations indicated that the shockwave and vapor micro-bubble expanded hemi-spherically on the glass surface. As shown in Fig. 4, formation and propagation of the shockwave and vapor micro-bubble were also observed upon laser irradiation at a fluence of 600 mJ cm^{-2} . This propagation was similarly monitored in the case of the aqueous dye solution [14].

Furthermore, the area of the laser irradiation on the silica glass corresponded to a bright square spot at the center of the images in Fig. 4. This visible emission was ascribed to the luminescence of toluene excited by KrF laser irradiation. The shadowgraph images of the shockwave and micro-bubble expansion were superimposed onto the luminescence image because our CCD-camera equipment was not equipped with a time-gated function. The time-integrated luminescence spectrum (Fig. 5) was ascribed to the emission of benzyl radicals [26], which were

mainly produced by the photochemical decomposition of toluene molecules by a single UV photon at 248 nm.

Masuhara and co-workers have reported that the threshold fluence for nanosecond-pulsed KrF excimer laser ablation of pure toluene was 35 mJ cm^{-2} in ambient air [26]. However, silica glass etching by the LIBWE method using toluene was observed above a fluence of 190 mJ cm^{-2} for KrF excimer laser. Therefore, at fluences between the two values, laser ablation would be insufficient for glass etching. Interestingly, upon the laser irradiation at 100 mJ cm^{-2} , two specific phenomena were observed using optical imaging. First, the formation of micro-bubbles was observed. The maximum size of the micro-bubbles at 100 mJ cm^{-2} was roughly $30 \mu\text{m}$ at a delay time of $5 \mu\text{s}$ ($V_{\text{jet}} = \text{ca. } 40 \text{ m s}^{-1}$), as shown in Fig. 6. Second, the shockwave was barely discernible using this imaging. These two observations are clearly distinct from the behavior upon laser irradiation above a fluence of 190 mJ cm^{-2} .

4. Conclusion

We demonstrated the $1 \mu\text{m}$ and $0.75 \mu\text{m}$ micro-structuring of silica glass etching via mask projection system of the LIBWE method. Since these microstructures were fabricated on $1 \text{ mm} \times 1 \text{ mm}$ areas, it is plausible that our methodology can be utilized in mass production. Although transient shockwaves and micro-bubbles induced by laser ablation of the solution expanded to the surroundings in the nano- and micro-second timescale (following laser irradiation), the well-defined micro-fabrications were successfully performed on the glass surfaces without any crack or debris formation. These results indicate that highly energetic states or species that can etch a silica glass surface possess

a short lifetime, with minimal influence outside the etched areas.

References

- [1] D. Bäuerle, *Laser Proces. Chem.*, third edition, Springer, Berlin, Heidelberg, 2000.
- [2] J. Ihlemann, B. Wolff, P. Simon, *Appl. Phys. A54* (1992) 363.
- [3] P.R. Herman, R.S. Marjoribanks, A. Oettl, K. Chen, I. Kononov, S. Ness, *Appl. Surf. Sci.* 154–155 (2000) 577.
- [4] K. Sugioka, S. Wada, H. Tashiro, K. Toyoda, A. Nakamura, *Appl. Phys. Lett.* 65 (1994) 1510.
- [5] J. Zhang, K. Sugioka, K. Midorikawa, *Opt. Lett.* 23 (1998) 1486.
- [6] J. Zhang, K. Sugioka, K. Midorikawa, *Appl. Phys. A67* (1998) 499.
- [7] H. Varel, D. Ashkenasi, A. Rosenfeld, M. Wähmer, E.E.B. Campbell, *Appl. Phys. A65* (1997) 367.
- [8] J. Wang, H. Niino, A. Yabe, *Appl. Phys. A68* (1999) 111.
- [9] J. Wang, H. Niino, A. Yabe, *Appl. Phys. A69* (1999) S271.
- [10] J. Wang, H. Niino, A. Yabe, *Jpn. J. Appl. Phys.* 38 (1999) L761.
- [11] J. Wang, H. Niino, A. Yabe, *Appl. Surf. Sci.* 154–155 (2000) 571.
- [12] Y. Yasui, H. Niino, Y. Kawaguchi, A. Yabe, *Appl. Surf. Sci.* 186 (2002) 552.
- [13] X. Ding, Y. Yasui, H. Niino, Y. Kawaguchi, A. Yabe, *Appl. Phys. A75* (2002) 437.
- [14] X. Ding, Y. Kawaguchi, H. Niino, A. Yabe, *Appl. Phys. A75* (2002) 641.
- [15] H. Niino, Y. Yasui, X. Ding, A. Narazaki, T. Sato, Y. Kawaguchi, A. Yabe, *J. Photochem. Photobiol. A: Chem.* 158 (2003) 179.
- [16] X. Ding, T. Sato, Y. Kawaguchi, H. Niino, *Jpn. J. Appl. Phys.* 42 (2003) L176.
- [17] X. Ding, Y. Kawaguchi, T. Sato, A. Narazaki, H. Niino, *Chem. Commun.* (2003) 2168.
- [18] Y. Kawaguchi, X. Ding, A. Narazaki, T. Sato, H. Niino, *Appl. Phys. A*, in press.
- [19] R. Böhme, A. Braun, K. Zimmer, *Appl. Surf. Sci.* 186 (2002) 276.
- [20] K. Zimmer, R. Böhme, A. Braun, B. Rauschenbach, F. Bigl, *Appl. Phys. A74* (2002) 453.
- [21] K. Zimmer, A. Braun, R. Böhme, *Appl. Surf. Sci.* 208–209 (2003) 199.
- [22] R. Böhme, D. Spemann, K. Zimmer, *Thin Solid Films* 453–454 (2004) 127.
- [23] G. Kopitkovas, T. Lippert, C. David, A. Wokaun, J. Gobrecht, *Microelectron. Eng.* 67–68 (2003) 438.
- [24] G. Kopitkovas, T. Lippert, C. David, A. Wokaun, J. Gobrecht, *Thin Solid Films* 453–454 (2004) 31.
- [25] Y. Tsuboi, H. Fukumura, H. Masuhara, *Appl. Phys. Lett.* 64 (1994) 2745.
- [26] Y. Tsuboi, K. Hatanaka, H. Fukumura, H. Masuhara, *J. Phys. Chem.* 98 (1994) 11237.